Pis'ma v ZhETF, vol. 74, iss. 11, pp. 625 – 629

Microscopic mechanism of stability in yttria-doped zirconia

S. A. Ostanin, E. I. Salamatov[+]

Department of Physics, University of Warwick, Coventry CV4 7AL, United Kingdom

[+]*Physico-Technical Institute, Ural Branch of RAS, 426001 Izhevsk, Russia*

Submitted 23 October 2001

The relaxed configurations of yttria-stabilised zirconia (YSZ) between 3 and 10 mol. % Y_2O_3 were modeled within the pseudopotential technique. In the displacive limit of the double-well potential model, the vibration mode corresponding to the soft phonon in pure c-ZrO_2 has been calculated for each Y_2O_3 composition. These anharmonic vibrations, associated with stabilization of YSZ, have been investigated within the self-consistent phonon approximation that makes obtainable the fine structure in spectral density. In studying the phonon dynamics, we propose to use the displacement probability density which can quantify very accurately the transition temperature needed to stabilize the YSZ cubic phase.

PACS: 63.20.-e, 64.70.Kb, 71.20.-b, 77.84.Bw, 81.05.Je

Yttria stabilized zirconia (YSZ), formed by the addition of Y_2O_3 into ZrO_2, is a controlling property material with numerous commercial applications [1]. Pure ZrO_2 exhibits three polymorphs: the monoclinic (m) phase, the tetragonal (t) phase between 1170 °C and 2370 °C and the high-temperature cubic (c) phase, which exists up to the melting point. Y_2O_3 has a large solid solubility range in ZrO_2 and can be used to stabilize the t-phase of $(Y_2O_3)_x(ZrO_2)_{1-x}$ over the composition range $0.02 < x < 0.09$ and the c-phase with $0.04 < x < 0.4$. In pure c- and t-ZrO_2, the Zr^{4+} ions are located in perfect and distorted 8-fold co-ordination environments, respectively, while, in m-ZrO_2, Zr^{4+} is found in 7-fold co-ordination. In YSZ, the trivalent dopant cations Y^{3+} substitute for some of the Zr^{4+} ions and, in order to maintain charge neutrality, one O vacancy (□) must be created for each pair of dopant cations. The presence of □s reduces the average cation co-ordination number to a value between 7 and 8 depending on the dopant concentration. YSZ contains relaxed defects such as □s and Y substituted atoms which make the local atomic enviroments of the stabilized crystals rather different from the corresponding stoichiometric phases.

Fig.1 shows the arrangement of atoms around the vacant O site before structural relaxation. The large cube in Fig.1 is the conventional fluorite unit cell with side of length a. It has been divided into eight octants and it is clear that the four NN 7-fold co-ordinated cations to the □ occupy the centres of alternate octants to create a tetrathedral arrangement around the vacancy. The t-distortion of the metal sub-lattice (∼1.03) has little effect on the relaxation process [2] and, therefore, it can be neglected. The nearest neighbour (NN) anion sites to the □ are located at the face-centres of the fluorite cube

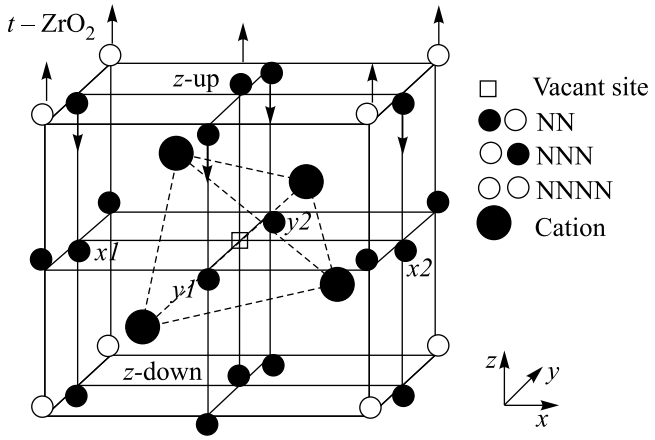

Fig.1. Unrelaxed arrangements of atoms in pure t-ZrO_2 near the vacant fluorite O site shown as a small empty box at the centre. The big circles, which form a tetrahedron, denote the ideal cation NN sites while the smaller circles denote the O NN (black), NNN (grey) and NNNN (light). The O NN atoms to the □ are labelled

while the anion next nearest neighbours (NNN) are positioned at the middle of each edge of the cube and the third nearest (NNNN) anions are at the corners. Fig.1 shows the initial t-distortion of the O sublattice with alternate columns of O, displaced up and down by $0.06a$ along the unique direction defined as [001].

To date, no full quantitative description of the stabilisation mechanism of YSZ has been reported. The X-ray absorption findings [3] confirm that dopant cations do not take an active part in stabilization. Using the *ab initio* technique to relax the c-cell, Stapper and coworkers [4] have reported that the NNN cation sites to vacancy rather than NN sites are favored for Y. Placing Y in the

NNN positions allows the coordination of Zr atoms in the NN sites to the □ to be similar to the arrangement in the m-phase while Y remains 8-fold co-ordinated. If the vacancies associate with host Zr ions, it may support a coordination-driven ordering model of stabilization in YSZ, which argues that increasing covalency lowers the co-ordination of Zr.

Recent neutron diffraction experiments report that at low concentrations of Y_2O_3 there are regions $\sim 15-20$ Å in size which contain isolated O □ and □s arranged in pairs on the NN anion sites in the [111] fluorite direction, with the cation site located between them occupied by Zr [5]. Modelling the long-range ordered $Zr_3Y_4O_{12}$ structure, Bogicevic et al. [6] have also reported that the □ pair along ⟨111⟩ and the 6-fold co-ordinated Zr appear in the most energetically favorable relaxed compositions. Electrostatic considerations suggest that □s should repel. From this point of view, the di-□ configuration along ⟨111⟩ would be favourable against those along ⟨100⟩ or ⟨110⟩. Because of the small size of Zr^{4+}, the electrostatic arguments place ZrO_2 on the border between the 8-fold co-ordinated fluorite and 6-fold co-ordinated structures [7]. The presence of the larger Y atoms, which possess the longer Y-O bond compared to the Zr-O bond, appears to shift this balance in favour of 7 fold and 6 fold coordination for Zr resulting in the local m- and brookite-type [8] bonds, respectively.

As for doped ZrO_2, no microscopic mechanism for the phase transitions has been proposed up to now. In pure ZrO_2, a zone-boundary soft phonon, X_2^-, which breaks the c-symmetry of the O sublattice, displacing the O atoms toward their positions in the t-phase, might be responsible for the $c \to t$ transformation. The previous calculations of the X_2^--phonon frequency within the harmonic approximation [2, 9] yield an imaginary frequency of 5.2–5.5 THz. This simply indicates the c-ZrO_2 is unstable at low temperatures. At high temperatures the effects of anharmonicity might stabilize the c-phase. Unfortunately, in YSZ, the experimental data [10] are not fully clarified for this soft mode because of the static disorders in the O sublattice. Thus, our theoretical investigation of the YSZ vibration mode which corresponds to the X_2^--phonon, would be useful in understanding a role of the atomic vibrations in this material. We believe that the allowance for anharmonicity can give a quantitative criterion to the microscopic mechanism of stability. In this approach, the "frozen-phonon" method [11] and self-consistent phonon approximation [12] are used to calculate the phonon frequency and its temperature dependence, respectively.

The plane-wave, pseudopotential based free energy molecular dymanics technique [13] is used to to relax the positions of atoms in the (96-y)-atom YSZ supercells (y=1,2,3) allowing to calculate the X_2^--phonon in YSZ between the 3 and 10 mol. % Y_2O_3 composition. The 95-atom cell corresponds to 3.2 mol. % Y_2O_3-ZrO_2. Starting from the c-configuration of O and experimental value of the unit cell volume, we make the static optimization allowing the co-ordinates of all atoms to be relaxed. Experimentally, 3 mol. % Y_2O_3-ZrO_2 can exist indefinitely in the t-form. The effect of starting relaxation with the O atoms in the t-geometry has been investigated as well showing the total energies reduced by $\sim$ 1 eV/cell relative to the relaxed c-configurations. The □ strongly prefers Y in NN sites before relaxation but, after relaxation, a configuration with two Y NNN shows the lowest energy. The energy differences between the different Zr/Y NNN configurations are only $\sim$ 1 meV/cation so that all are likely to co-exist in this material at room temperature.

The 94- and 93-atom cells model 6.7 and 10.4 mol. % Y_2O_3-ZrO_2. Placing Y not closer than NNN site to each □, an optimum configuration has been obtained. In the lowest energy configuration of the di-vacancy cell, the □s are along the fluorite [111] direction and separated by the 6-fold co-ordinated Zr. This brookite-type Zr-O motif sometimes can appear in the low-energy configurations of the high Y_2O_3 compositions. Fig.2, in panel (a), shows the difference in energy between the most

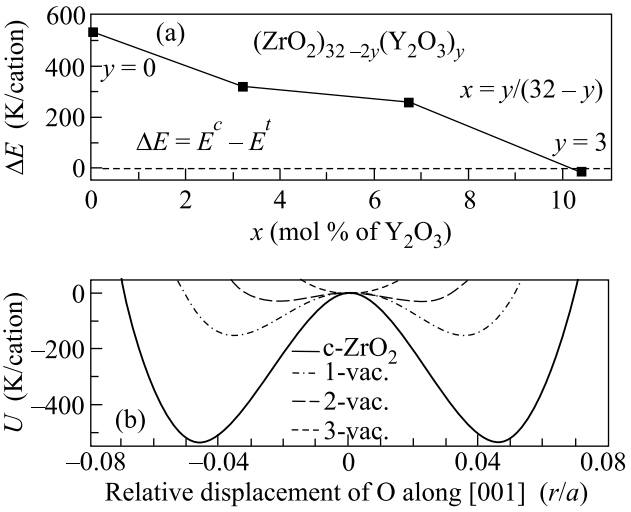

Fig.2. Difference in the relaxed energy between the t- and c-configurations of YSZ, is shown in panel (a). In panel (b), a decay of the double-well potential, with yttria doping, is shown as the change in energy plotted vs the t-displacements of the O sublattice for each concentration of Y_2O_3

stable c- and t-configurations. The energy is given in Kelvin per cation to show the temperature required. In the mono- and di-□ cells, the t-configurations are more stable while, for 3-□s, the c-configuration is marginally more stable. Experimentally, the same change in stability is observed.

The experimental electron energy-loss near-edge shapes (ELNES), which depend on the crystal structures and the Y_2O_3 composition, can be a characterization probe of this doped oxides. *Ab initio* calculations [8] were performed to obtain the O K-edge ELNES in the relaxed YSZ demonstrating that relaxation of defects plays an important role. Good agreement between calculated and measured ELNES data were obtained with respect to the number of maxima, the intensity ratios and energy positions of the peaks [8]. This agreement shows that our modelling can reflect the realities of YSZ.

Within the "frozen phonon" method, the effective phonon potential can be calculated as the difference in energy between the perfect and distorted lattices for various amplitudes of atomic displacements maden accordingly the symmetry of the phonon considered. In doped ZrO_2, the intrinsic defects break the translation symmetry and therefore one has to deal with the renormalized phonon whose attenuation is due to the scattering on these defects [14]. Fig.2, in panel (b), displays the effective potential U, calculated as a function of the O t-displacements, r/a, along the z-axis. The Us were shifted to the common zero energy at r=0 to illustrate the development of a double-well shape. In 10 mol. % Y_2O_3, U has a single minimum at r=0. With decreasing Y_2O_3 content, U develops two minima i.e. its form becomes similar to that of the X_2^- phonon in pure c-ZrO_2. The relative temperature units used give an idea of the temperature changes of the $c-t$ interface. In fact, for practical calculations, the Us should be normalised per fluorite (4-cation) unit cell.

The modified pseudoharmonic approximation [12] has been developed to calculate anharmonic dynamics of the quasi-local mode associated with the low-frequency vibrations of the defective atoms. This model has been applied recently to study the structure instability in pure Fe [15] and Zr [16]. In the present work we consider the one-phonon inelastic neutron scattering spectrum, whose peak position and width determine the phonon frequency and lifetime. The spectral intensity can be calculated via the imaginary part of the one-phonon Green function, spectral density $g_q(\omega, T)$ [14]:

$$I_q(\omega, T) \sim g_q(\omega, T) = \frac{1}{\pi} \frac{\Gamma(\omega_q, T)}{(\omega - \tilde{\omega}_q(T))^2 + \Gamma^2(\omega_q, T)}, \quad (1)$$

where $\tilde{\omega}_q(T)$ is the renormalized frequency and $\Gamma(\omega_q, T)$ is the phonon attenuation due to various scattering processes. For the latter we restricted ourselves to the defect-dependent attenuation: $\Gamma(\omega, E) = A_x \omega(E)$, with $A_x = 0.1, 0.15, 0.2, 0.25$ for each $x = 0, 1, 2, 3$ concentration of Y_2O_3. A random variable E, the energy averaged over characteristic period of oscillations, can be introduced [12] with its mean value $< E >= T$ and equilibrium distribution function $\rho(E) = \exp(-E/T)/T$. The characteristic time of variation of E is $\tau_E \sim 1/\Gamma \gg 1/\omega_q$ i.e. this variable is slow, as compared to the oscillation period, that allows us to calculate the frequency for each E within the pseudoharmonic approximation [12]. The partial density $g_q(\omega)$ can be obtained by averaging Eq. (1) (where the substitution of E for T is maden) with distribution function $\rho(E)$.

The result might be resumed as follows: at all temperatures, there is an occasion to find (i) the basic (b) vibrations localized near minima of U, with the frequencies ω_b close to the principal frequency ω_0 ($m\omega_0^2 = \partial^2 U(r)/\partial r^2 \mid_{r=r_{min}}$), and (ii) the excited (e) over-barrier vibrations with $\omega_e \simeq \omega_0/2$. With increasing temperature, the portion of the b-vibrations diminishes $c_b = 1 - \exp(-E_c/T)$ (E_c is the "local transition" energy [12]) while the share of e-vibrations increases $c_e = 1 - c_b$. New harmonics therewith arise, which lead to a shift of the peaks and some changes of their anharmonic broadening. The basic vibration peak moves towards the low-frequency range while the e-peak moves towards the high-frequency range. These findings are in qualitative agreement with previous numerical results [17] which describe the anharmonic mode dynamics using the arbitrary potential and oscillator attenuation.

In pure ZrO_2, the $g_q(\omega)$ plotted in panel (a) of Fig.3 shows the b-peak at room temperature as if it would be in the t-phase. At intermediate temperatures, the b-peak and e-peak are clearly resolved. With increasing temperature, the intensity of the b-peak falls and, finally, at $T = 3000$ K the cubic-like e-vibrations become dominant. In pure material, the calculated ω_e of ~ 10 THz is rather reasonable value compared to the acoustic phonon branches observed in this point of the Brillouin zone [10]. Fig.3, in panel (b), shows the $g_q(\omega)$s at T=1000 K. At this temperature the b-vibrations are dominant in pure ZrO_2 exclusively. In YSZ, the $g_q(\omega)$s, shown in this panel for each defective cell, illustrate the evolution in shape with increasing Y_2O_3. This fine structure in the $g_q(\omega)$ shape of the soft phonon, responsible for the $c \to t$ phase transition in YSZ, indicate that both these phases may co-exist at intermediate temperatures.

Since, within the framework of the method used, the arbitrary parameter $\Gamma(\omega, E)$ cannot be estimated it

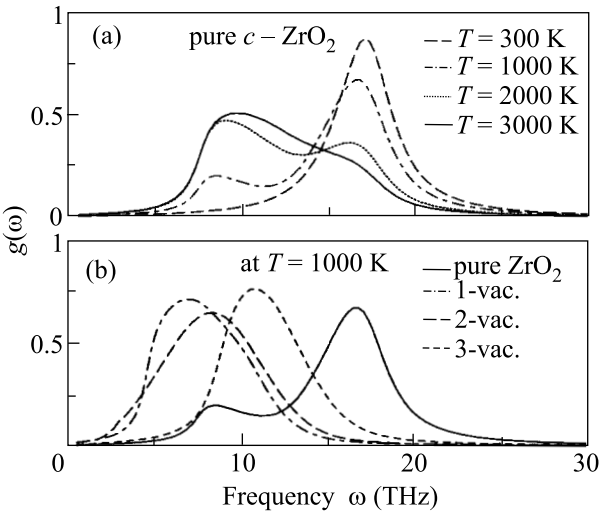

Fig.3. Spectrum of the soft phonon mode in pure c-ZrO_2 at different temperatures, plotted in panel (a), and its changes in YSZ with yttria doping, which are shown in panel (b)

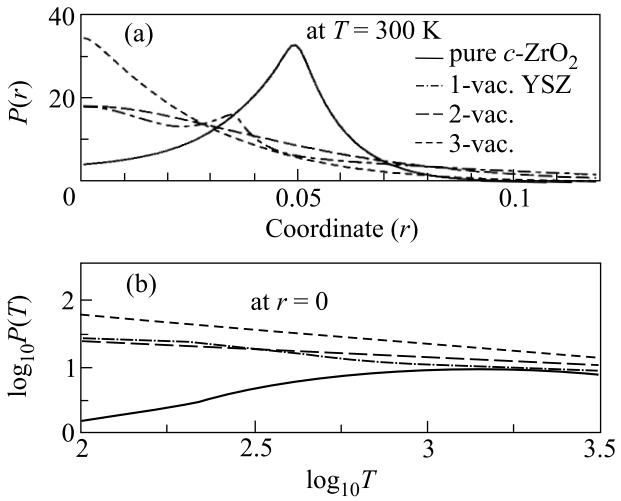

Fig.4. The displacement probability densities $P(T, r)$: the room-temperature Ps ranging between 0 and 10 mol. % Y_2O_3, which are plotted in panel (a), and the zero-coordinate Ps, shown in panel (b)

would be desirable to consider a $\Gamma(\omega, E)$-independent function other than $g_q(\Gamma)$. It might be the displacement probability density [18] (DPD):

$$P(r) = \int P_{\rm harm}(r, E)\, \rho(E)\, dE\,, \qquad (2)$$

where

$$P_{\rm harm}(r, E) = \sqrt{\frac{C(E)}{2\pi}}\, \exp\left\{\frac{-[r - r_0(E)]^2\, m\omega^2(E)}{2k_B E}\right\}, \qquad (3)$$

and $C(E) = m\omega^2(E)/k_B E$. In panel (a) of Fig.4, the DPD, plotted for pure and defective zirconias, display the change in the $P(r)$-shape at room temperature. In pure ZrO_2 and single-vacancy YSZ, the DPD shows the peak in the region of the b-vibrations that illuistrates the room-temperature instability of the c-configuration. The temperature dependence of DPD at r=0 is shown in panel (b). In the di- and tri-□ cells, the $\log_{10} P$ vs $\log_{10} T$ at r=0 is almost linear showing the decreasing trend with increasing temperature. In pure ZrO_2 and 3 mol. % ZrO_2-Y_2O_3, there is the low temperature peak of $\log_{10} P_{r=0}$ and then, with increasing temperature, the linear behaviour against $\log_{10} T$ appears. In ZrO_2, such form of DPD starts at ~2500 K i.e. close to the $t \to c$ transition temperature observed whereas the 3 mol. % Y_2O_3 shows the room temperature characteristic value. Note, that at this point, the lattice dynamics become unchangeable with variation of $U(r)$ near its bottom ($T \gg E_b$).

In summary, the calculated DPD features of YSZ are in very good agreement with experiment. This fact suggests that the zero-coordinate DPD, $P_{r=0}(T)$, can be used as a quantitative criterion of stability in zirconia-stabilized materials. The report can be considered as a first attempt to get some insight whether the t- and c-phases can co-exist in YSZ. It would be worthwhile to apply this model to investigate the low temperature stability in other doped metal oxides.

We wish to thank Mike Finnis, Alan Craven and Ali Alavi for their encouraging interest in this work. E.S. thanks Russian Fondation for Basic Research (grants # 01-02-96463 and # 00-02-17426) for financial support.

1. E. C. Subbarao, in *Science and Technology of Zirconia*, Eds. A. H. Heuer and L. W. Hobbs, *Advances in Ceramics*, Vol. 3, American Ceramic Society, OH, 1981.
2. S. Fabris, A. T. Paxton, and M. W. Finnis Phys. Rev. **B63**, 94101 (2001).
3. P. Li, I-Wei Chen, J. E. Penner-Hahn et al., Phys. Rev. **B48**, 10063 (1993); **48**, 10082 (1993).
4. G. Stapper, M. Bernasconi, N. Nicoloso, and M. Parinello, Phys. Rev. **B59**, 797 (1999).
5. J. P. Goff, W. Hayes, S. Hull et al., Phys. Rev. **B59**, 14202 (1999).
6. A. Bogicevic, C. Wolverton, G. M. Crosbie, and E. B. Stechel, Phys. Rev. **B64**, 14106 (2001).
7. M. W. Finnis and A. T. Paxton, Phys. Rev. Lett. **81**, 5149 (1998).
8. S. Ostanin, A. J. Craven, D. W. McComb et al., Phys. Rev. **B62**, 14728 (2000).
9. F. Detraux, Ph. Chosez, and X. Gonze, Phys. Rev. Lett. **81**, 3297 (1998).

10. D. W. Liu, C. H. Perry, A. A. Feinberg, and R. Currat, Phys. Rev. **B36**, 9212 (1987); D. N. Argyriou and M. M. Elcombe, J. Phys. Chem. Solids **57**, 343 (1996).
11. Y.-Y. Ye, Y. Chen, K.-M. Ho, B. N. Harmon, Phys. Rev. Lett. **58**, 1769 (1987).
12. E. I. Salamatov, Phys. Stat. Sol. **(b)197**, 323 (1996); **177**, 75 (1993).
13. A. Alavi, J. Kahonoff, M. Parrinello, and D. Frenkel, Phys. Rev. Lett. **73**, 2599 (1994).
14. A. A. Maradudin and A. E. Fein, Phys. Rev. **128**, 2589 (1962).
15. S. A. Ostanin and E. I. Salamatov, J. Phys.: Condens. Matter. **9**, 37063 (1997).
16. S. A. Ostanin, E. I. Salamatov, and V. Yu. Trubitsin, Phys. Rev. **B57**, 5002 (1998); **58**, R15962 (1998).
17. Yu. N. Gornostyrev, M. I. Katsnelson, A. V. Trefilov et al., Phys. Rev. **B54**, 3286 (1996); C. A. Condat and P. W. Lamberti, Phys. Rev. **B53**, 8354 (1996).
18. S. Aubry, J. Chem. Phys. **62**, 3217 (1975).